Hindawi
Journal of Energy
Volume 2018, Article ID 4303580, 11 pages
https://doi.org/10.1155/2018/4303580

*Research Article*

# Modeling, Analysis, and State Feedback Control Design of a Multizone HVAC System

**Almahdi Abdo-Allah**,[1] **Tariq Iqbal**,[1] **and Kevin Pope**[2]

[1]*Department of Electrical and Computer Engineering, Memorial University of Newfoundland, St. John's, NL, Canada A1B 3X5*
[2]*Department of Mechanical Engineering, Memorial University of Newfoundland, St. John's, NL, Canada A1B 3X5*

Correspondence should be addressed to Almahdi Abdo-Allah; atmaa7@mun.ca

Received 26 October 2017; Accepted 6 March 2018; Published 9 May 2018

Academic Editor: Ahmed Al-Salaymeh



A HVAC system is modeled by applying a state space MIMO (multi-input/multioutput) system method for control system design and analysis. Thermal models are developed using the simulation program IDA Indoor Climate and Energy. The building has four floors in total, with separate air-handling units (AHUs) on each floor. The system's eight main input data are hot water and the energy usage for each AHU, while the eight main outputs are return airflow temperature and $CO_2$ levels for AHUs. The factors of wind direction and velocity are also applied as disturbances. By comparing usage data on simulated power consumption versus measured data for the three months of October, November, and December 2016, good agreement was achieved with simulated data. The main aim is to develop a state feedback controller and then apply it toward optimal functionality of a control system. After utilizing the MATLAB identification toolbox, a MIMO system-based state space model is developed.

## 1. Introduction

A main aim in developing an optimal HVAC (heating, ventilation, and air-conditioning) system is to create a comfortable environment for occupants with reduced energy inputs [1]. However, heating and cooling loads typically change according to the exterior environment, as well as with the specific needs of the users. HVAC systems require a control system to keep the comfort level and air quality relatively constant with variable conditions. Furthermore, power usage can be greatly decreased if the system is suitably controlled.

A method that is based solely on measured data is one possible means for obtaining a mathematical interpretation of the system. The model can be used to determine system parameters in cases where input and output variables are already available. This modeling method is useful if the system is constructed and data related to performance can be readily obtained. Compared to forward models, those that are data-driven can identify system approaches that can prove to be both easier to use and better performance predictors. Modeling methods that primarily use data are classified as "system identification" (ASHRAE 2005).

A wide range of research over the past few decades supports the suitability of applying the system identification approach in energy simulation and in determining and analyzing the moisture, cooling, and heating environments in buildings. Applying data gathered from a building management system, Lowry and Lee (2004) studied the outcome of using a data-driven model to gauge thermal response [2]. A few years earlier, Madsen and Holst (1995) utilized nearly the same system identification approach to determine a structure's heating dynamics obtained from data on discrete time performance [3]. Cunningham (2001) applied system identification methods to find moisture release rates in a structure based on psychometric data [4], and Mechaqrane and Zouak (2004) incorporated system identification in their investigations on the prediction of interior air temperature in residential structures [5]. A few studies have also focused on comparing test approach models with theoretical predictions using simulation software like TRNSYS. Peippo et al. (1991) determined the dynamics of a structure according to discrete time results obtained from simulation software using a one-hour time step [6].

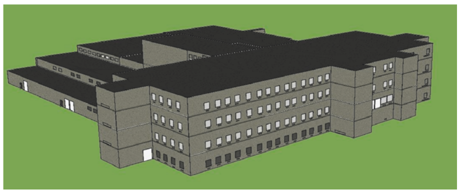

Figure 1: 3D model of the S. J. Carew building using IDA Indoor Climate and Energy program.

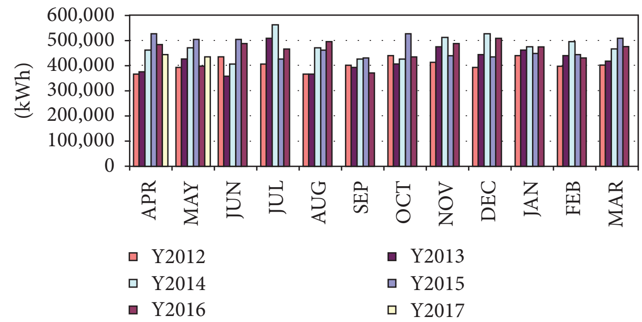


Figure 2: Power usage for the whole building from April 2012 to May 2017.

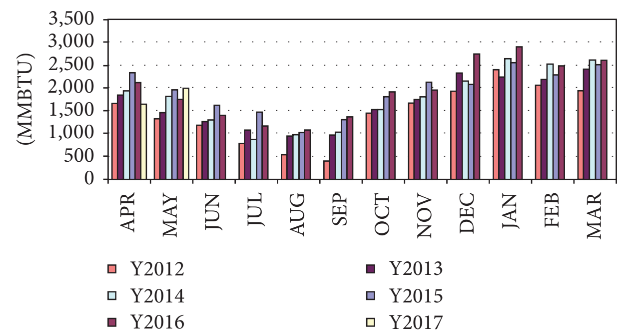


Figure 3: Hot water usage for the whole building from April 2012 to May 2017.

Despite the approach's clear potential, there are numerous obstacles to the simulation of a structure's dynamic response when applying simulation software. Currently, simulation software can be significantly time-consuming and the results are often missing important information on the fast dynamic behavior of a structure (i.e., in the order of seconds), as the majority of available software utilizes a discrete time step that is typically set at one hour. Problems arise when, for instance, data is needed on fast dynamic behavior for a control strategy (e.g., on/off), but it cannot be obtained because it is situated within the time step.

This paper presents a simulation of an entire structure, applying the simulation program IDA Indoor Climate and Energy 4.7. The energy usage (including heating and cooling) of the S. J Carew Building of Memorial University of Newfoundland is investigated with a 3D numerical model using IDA ICE software. Established in 1998, the IDA Indoor Climate and Energy program can investigate separate thermal climate zones [7]. There are four main objectives of the present work:

(1) Use real data to create entire structure and then validate the results.

(2) Determine the viability of using system identification in decreasing the time required for calculating the simulation of complex structures.

(3) Determine the viability of using system identification for identifying the dynamics of climate control design in a structure when using discrete time data of one-hour sample time.

(4) Use state feedback (classical) control by applying a state space model.

## 2. Building Thermal Simulation

*2.1. Building Structure.* For analysis purposes, a building is located on the Memorial University campus in St. John's, Newfoundland and Labrador. The structure is the S. J. Carew Building, which accommodates Memorial's Faculty of Engineering and Applied Science. There are more than 300 zones in the S. J. Carew building, which measures approximately 25,142 m$^2$ and comprises a cafeteria, teaching rooms, staff rooms, and research labs. Table 1 provides a description of the structure's amenities and Figure 1 illustrates the structure.

Initially, a section of the building is investigated using the simulation software IDA ICE [7]. Data is applied on the weather for St. John's and also construction details (e.g., windows, doors and walls, and radiators, fans, and pumps) to obtain energy consumption information for the simulation. In addition, we apply AutoCAD files drawings for determining the dimensions of the building such as the height of the building, size and positions of the windows and doors, and information on ventilation and heating systems.

*2.2. IDA ICE Simulation Validation.* Determining whether the model satisfies the requirements and whether the results are accurate is critical to developing a feasible model. In this study, data is obtained from the Department of Facilities Management at Memorial University and compared with the structure's hot water and power usage. Figure 2 illustrates the power usage and Figure 3 illustrates the hot water for the entire structure of the S. J. Carew building from April 2012 to May 2017.

Table 2 and Figure 4 illustrate the IDA ICE data for three months, October to December 2016, including energy consumption in the building, from lighting, HVAC, and equipment, such as computers, TV, cookers, and fridge-freezer.

The output variables of exterior temperature, hot water power usage, and power usage are compared with simulation data (three months' worth) from IDA ICE software, as follows.

*2.2.1. Exterior Temperature.* Exterior temperature from the IDA ICE program and data weather files were compared with data from October to December 2016, using one-hour time samples, as shown in Figure 5.

Table 1: Details of the building.

| Equa. Simulation technology group Project | | Delivered energy report Building | |
|---|---|---|---|
| | | Model floor area | 25141.7 $m^2$ |
| Customer | | Model volume | 128952.9 $m^3$ |
| Created by | Almahdi Abdo-Allah | Model ground area | 10544.5 $m^2$ |
| Location | Newfoundland (St. John's Airport) _718010 (ASHRAE 2013) | Model envelope area | 29440.0 $m^2$ |
| Climate file | CAN_NF_St. Johns.718010_CWEC | Window/Envelope | 2.40% |
| Case | building2017_AHU8. | Average $U$-value | 0.3031 W/($m^2$ K) |
| Simulated | 2/13/2017 23:03 | Envelope area per Volume | 0.2283 $m^2/m^3$ |

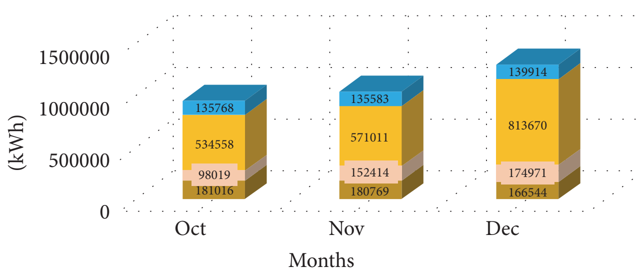


Figure 4: IDA ICE data for three months (October to December 2016).

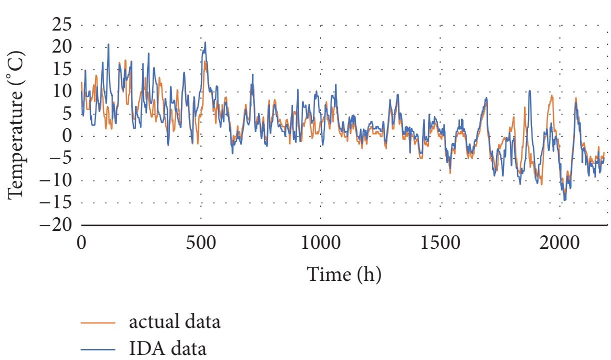


Figure 5: Difference between outdoor temperatures of IDA ICE and actual data.

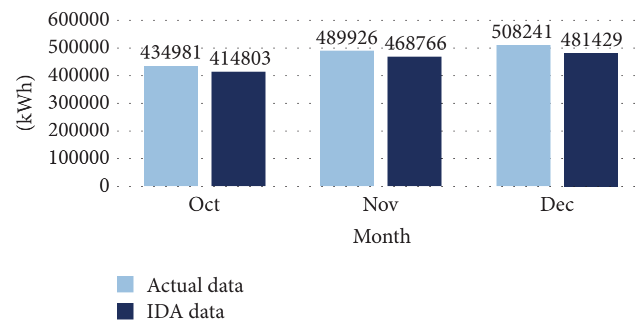


Figure 6: Difference between power usage of IDA ICE and actual data.

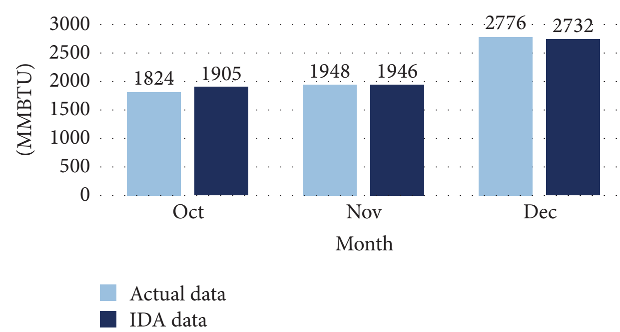


Figure 7: Difference between hot water power usage of IDA ICE and actual data.

*2.2.2. Power Usage.* The modeled data differs slightly from measured data for power usage. As illustrated in Figure 6 the measured data slightly exceeds the modeled data, which is likely due to differences in laboratory equipment.

*2.2.3. Hot Water Power Usage.* As illustrated in Figure 7, in October to December 2016 IDA ICE model, hot water power usage measured 6,583 MMBTU. Hot water usage in October for actual data was lower than IDA data, but in December was opposite and November was almost the same.

*2.3. Simulation Model.* The IDA Indoor Climate and Energy 4.7 (IDA ICE) simulation tool is used to make an assessment on both the energy performance and interior climate. The tool can model multiple-zoned structures housing HVAC and can also be used for assessing thermal comfort, interior air quality, dynamic simulation, and required energy. Figures 9, 10, and 11 provided details on the zonal input and output data. This information is needed for the identification data and reference model for modeling the building.

## 3. System Identification

Three distinct stages can be defined when using system identification [8]:

(i) Data gathering for identifying the model.

(ii) Choosing a suitable model structure.

(iii) Developing a model which offers optimal system functionality.

Table 2: IDA ICE data for three months (October to December 2016).

| Month | Facility electric Lighting, facility (kWh) | Facility electric HVAC aux (kWh) | Facility fuel (heating value) Domestic hot water (kWh) | Tenant electric Equipment, tenant (kWh) | | Purchased energy kWh | Purchased energy kWh/m$^2$ | Peak demand kW |
|---|---|---|---|---|---|---|---|---|
| | | | | | Lighting, facility | 548329 | 21.8 | 251.1 |
| Oct | 181016 | 98019 | 534558 | 135768 | HVAC aux | 518404 | 20.6 | 460.2 |
| Nov | 180769 | 152414 | 571011 | 135583 | Domestic hot water | 1919239 | 76.1 | 2610 |
| Dec | 166544 | 174971 | 813670 | 139914 | Equipment, tenant | 411265 | 16.4 | 188.3 |
| Total | 528329 | 425404 | 1919239 | 411265 | | | | |

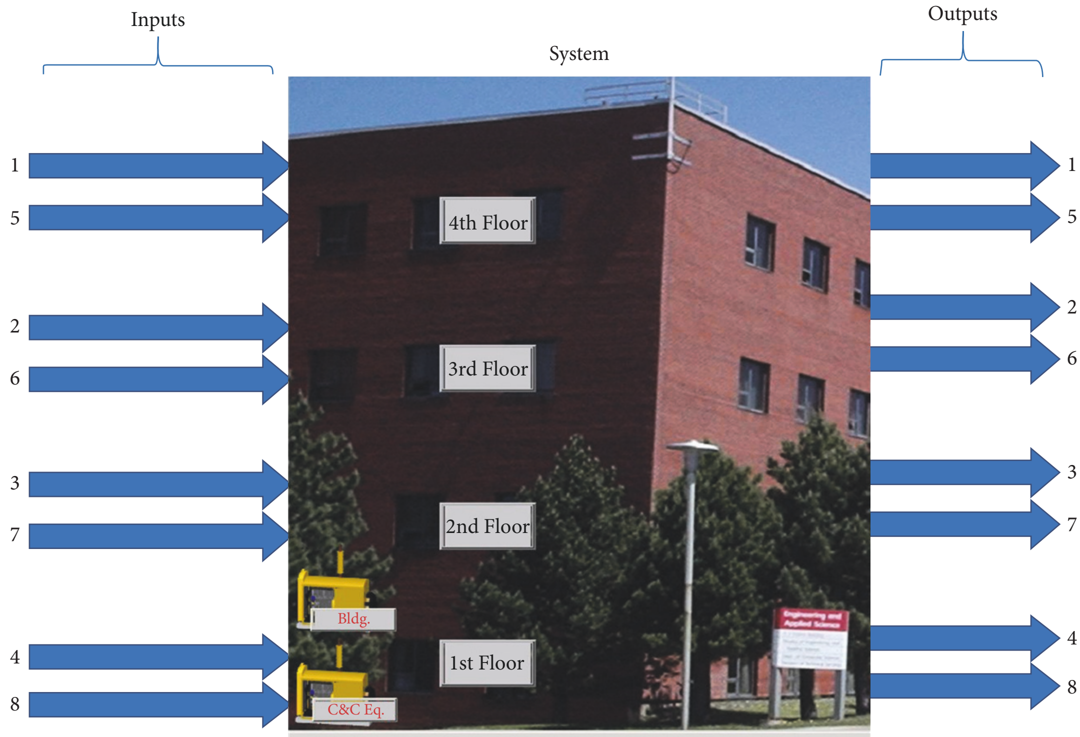


Figure 8: System with eight inputs and eight outputs.

The S. J. Carew building has four AHUs which are needed to identify the system's state space model. The system has eight inputs; 1, 2, 3, and 4 represent the hot water power usage (kWh) and 5, 6, 7, and 8 represent the power usage (kWh) inputs of the system. The outputs, 1, 2, 3, and 4 represent the level of $CO_2$ (PPM), while the 5, 6, 7, and 8 outputs represent the zone temperature (°C), as shown in Figure 8.

*3.1. Input Signals.* A rise in airflow temperatures and radiator heat of the zonal temperature and hot water flow (minimum and maximum temperatures) is highly plausible. These form the zones' sole control variables; thus identification system signals can be used as input signals. The system's power usage (PU) and hot water power usage (WPU) as a time function, for each AHU, are illustrated in Figure 9.

*3.2. Output Signals.* The system outputs are defined as the temperature and $CO_2$ level in the return air flow. Returned air $CO_2$ levels are shown in Figure 10 and returned air temperature variations are shown in Figure 11.

*3.3. Choosing a Model Structure.* A model structure is selected from range of structures which are roughly categorized as being either linear or nonlinear. However, because we are using a nonlinear system in this work, we choose the ARMAX model.

*3.4. Identifying the Model.* For the identification decision process used in preprocessing the data, the decision process can be categorized into five stages [9]:

(a) Deciding the optimal model structure (e.g., ARX, ARMAX, and process models) for our purposes.

(b) Deciding the model order.

(c) Deciding the optimal estimation approach.

(d) Launching the identification process.

(e) Reviewing and validating the results.

*3.5. State Space Model.* The total quantity of the system's independent components is assumed equal to the total number of the state variables, $n$. The system's total power and state time derivative variables set the system's power change rate, and the system's state variables, at time, $t$, give enough data for calculating the values of the system's variables for that time [10]. The multizone HVAC system was developed as single system with 42 states and nine outputs [11, 12].

$$\dot{x} = Ax + Bu$$
$$y = Cx + Du. \tag{1}$$

Matrix $A_{8*8}$ and matrix $B_{8*8}$ form the system's properties. Hence, the output variables impact the output equation matrices ($C_{8*8}$ and $D_{8*8}$). The matrices are calculated by applying the MATLAB tool box for system identification.

Additionally, using MATLAB, we can formulate the system's dynamic behavior for an arbitrary input and *lsim (sys, u, t, xo)* function simulation. The system uses eight inputs, each depicted as $u$, while the time samples are given as *t vector* and $x_o$ indicates the system's starting values. The system

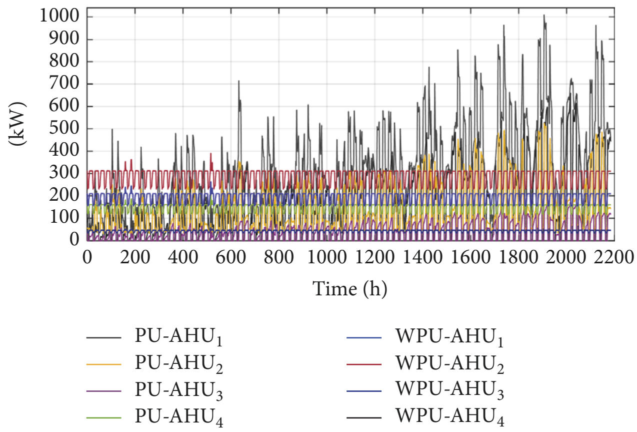


Figure 9: Actual data of power usage (PU) and water power usage (WPU) of the building, for each AHU.

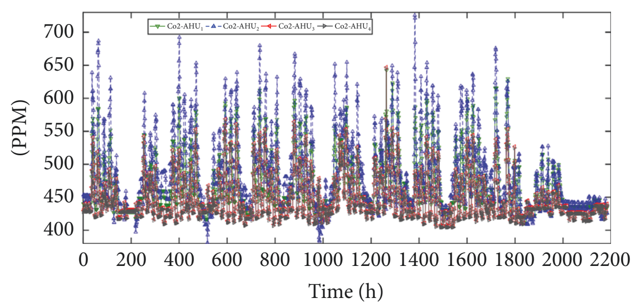


Figure 10: Actual data of return air $CO_2$ levels of the building for each AHU.

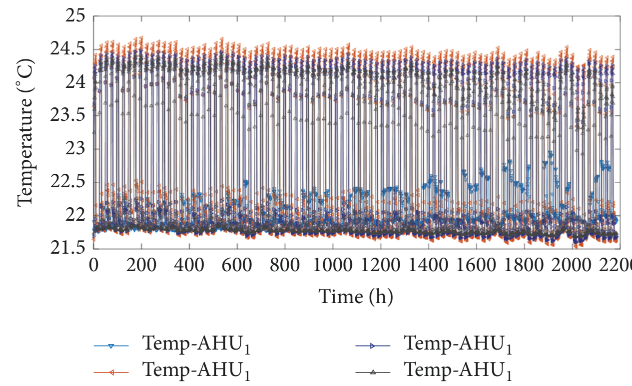


Figure 11: Actual data of return air temperature of the building for each AHU.

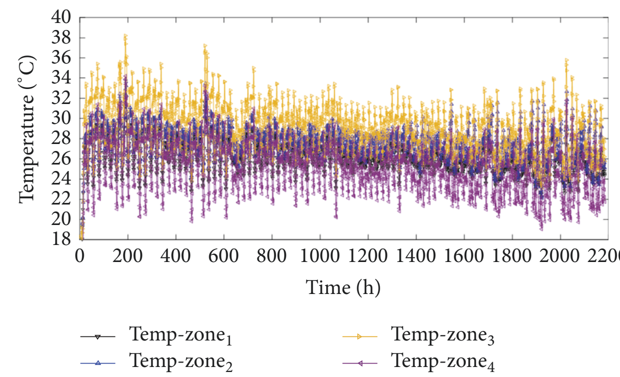


Figure 12: System outputs response zonal mean temperatures using *lsim (sys, u, t, xo)* function simulation.

outputs response, in Figure 12, shows the zonal temperatures, while Figure 13 indicates the zonal level of $CO_2$.

As illustrated in Figure 13, the system responses fall within the correct range if the starting transient is neglected.

## 4. Control Strategies

HVAC systems control interior environmental factors such as room humidity and temperature in commercial or residential structures, with the overall aim of giving users a comfortable working and living environment. HVAC systems are so widely used that they comprise at least 50% of global power usage [13–16]. In addition to creating a comfortable working and living environment, HVAC controls typically need to also consider maximizing energy efficiency. System identification and state space model for one AHU of the S. J. Carew Building was presented without control [17]. In earlier studies, researchers investigated mainly humidity and temperature levels in modeling HVAC systems [18–22]. A nonlinear HVAC model was introduced [18, 19] that involves a temperature/humidity ratio and an observer for determining approximate moisture and thermal loads. An adaptive fuzzy output feedback controller was developed [20] that can be premised on an HVAC system observer. Researchers proposed applying both a decentralized nonlinear adaptive controller [21]. and a back-stepping controller [22] on a model.

$CO_2$ concentrations are generally seen as having a notable impact on room comfort levels [23, 24]. Accordingly, some researchers are suggesting developing a hybrid HVAC system that can develop temperature continuous states, as well as $CO_2$ concentration as a discrete state [25, 26]. As these states can be highly interrelated, a more viable approach would be to integrate the presented discrete and continuous dynamics to form a model that assumes $CO_2$ concentration and temperature as states.

A system's possible future development can be predicted by the state of a dynamical system, the latter is essentially a group of variables. The control system is used to bring the nonlinear system into a stable state, while achieving the control targets. For one AHU unit system design feedback linearization technique has been applied [27]; the control of the cross-water heat exchanger [28] and feedback controller achieves global input-output linearization of greenhouse environments [29]. In creating system dynamics by referring to state feedback, the multi-input system can be controlled as a linear state model. Hence, the feedback control can be devised through a step-by-step process that is based on putting closed loop eigenvalues in specific places. Figure 14 illustrates a control system that utilizes state feedback. The system which features linear process dynamics, processes disturbances, $d$, reference input, $r$, and controller elements,

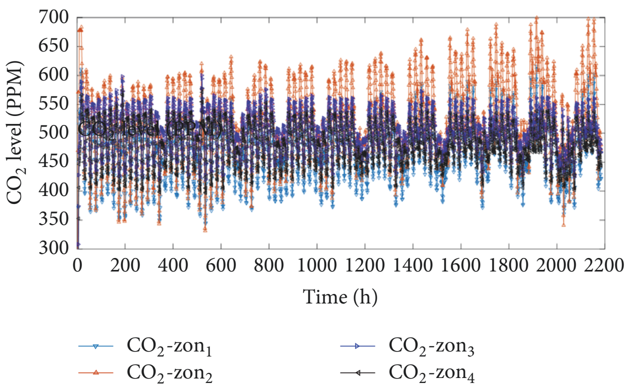

FIGURE 13: The system outputs response zonal $CO_2$ level using *lsim (sys, u, t, xo)* function simulation.

$K$, is feedback gain and $K_r$ is input gain. The feedback controller's main purpose is regulating the system output, $y$, until it tracks the reference input during process dynamics uncertainty and disturbances.

Performance specifications are critical to control design and the most important feature is stability. The aim is for the system's equilibrium point to stabilize asymptotically, but increasingly complex specifications can include obtaining the preferred properties from the system's step or frequency responses. Such desired specifications include rise times, overshoot, and settling times of step responses. In optimizing functionality, the system's disturbance rejection properties can be analyzed to find the best way to handle disturbance inputs, $d$, while maintaining output, $y$, at the required value specifications.

The system is represented by the following linear differential matrix equation:

$$\begin{aligned} \dot{x} &= Ax + Bu \\ y &= Cx + Du. \end{aligned} \tag{2}$$

It is assumed that $D = 0$ while neglecting the disturbance signal, $d$. The aim is to give the output a value, $r$. In this scenario, state vector components must first be calculated. Thus, as the state at time, $t$, already has the required data for predicting the system's behavior, the following time invariant control law becomes both a state function and reference input:

$$u = \alpha(x, r). \tag{3}$$

The equation can be formulated as follows, if the feedback is maintained linear:

$$u = -Kx + K_r r. \tag{4}$$

In this equation, the reference value, $r$, has been deemed constant, which refers back to Figure 14. Here, the negative sign works as an indicator of negative feedback being standard procedure. The closed loop system which we created after the feedback (2) has been applied to the system (4) can be calculated as

$$\frac{dx}{dt} = (A - BK)x + BK_r r. \tag{5}$$

To find feedback gain, $K$, to set the characteristic polynomial of the closed loop system:

$$p(s) = s^n + p_1 s^{n-1} + \cdots + p_{n-1}s + p_n. \tag{6}$$

This formulation is known as the "pole placement" or eigenvalue assignment problem. In the formulation, $K_r$ input gain has no effect on system stability (the latter is instead created by $A - BK$ eigenvalues) but does have an impact on the steady state solution. Thus, we can set the equilibrium point and steady state output as

$$\begin{aligned} x_e &= -(A - BK)^{-1} BK_r r \\ y_e &= Cx_e. \end{aligned} \tag{7}$$

In this formulation, $K_r$ is the best choice, which then gives $y_e = r$, which is the required value. Furthermore, because $K_r$ is scalar:

$$K_r = \frac{-1}{\left(C(A - BK)^{-1}B\right)}. \tag{8}$$

The variable $K_r$ represents the opposite of the closed looped system's zero-frequency gain. Therefore, by applying $K_r$ input gain and $K$ which is $(8 \times 8)$ feedback gain matrix, the dynamics of a closed loop system can be modified until the required specifications are achieved. In this paper, the state feedback gain matrix is

$$\begin{bmatrix} 102080.4 & -93791.2 & -729047 & 614999.7 & 350096.8 & 658615.9 & 202011.9 & 30447.25 \\ -1446580 & 596078 & -969369 & 776114.2 & 1646412 & 355322.9 & -393128 & -50502.8 \\ 645753.8 & -269577 & -1935998 & 1784298 & 589759.8 & 821055.8 & 623924.2 & 91440.54 \\ 388775.7 & -184664 & -601331 & 542196.5 & 197042 & 354662.3 & 191710.6 & 27060.44 \\ -30.043 & 25.90427 & 20.8471 & 0.886393 & 20.65468 & -3.9515 & -7.54395 & -0.83403 \\ -39.3176 & 33.88056 & 27.27797 & 1.154438 & 27.0208 & -5.17458 & -9.88601 & -1.0934 \\ -58.262 & 50.20904 & 40.42217 & 1.711219 & 40.04134 & -7.66779 & -14.6487 & -1.6203 \\ -8.83168 & 7.630466 & 6.129845 & 0.253818 & 6.062056 & -1.17064 & -2.24588 & -0.24996 \end{bmatrix}. \tag{9}$$

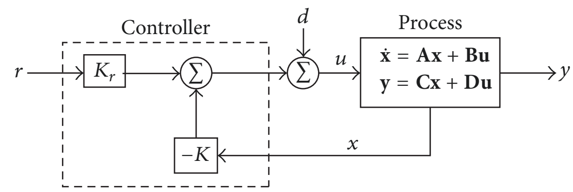


FIGURE 14: Block diagram of a system with state feedback ($K$) and input $K_r$ controllers.

## 5. Simulation Results

*5.1. Open Loop System.* The system has eight inputs and eight outputs. In this part, the system is presented by 64 transfer functions each relating one input to one output.

$$
\begin{aligned}
G_{11} &= \frac{y1}{u1} = \frac{-0.024s^7 + 0.009s^6 - 0.03s^5 + 0.067s^4 - 0.107s^3 + 0.127s^2 - 0.08s + 0.027}{s^8 - 3.55s^7 + 6.323s^6 - 7.5s^5 + 6.66s^4 - 4.711s^3 + 2.635s^2 - 1.06s + 0.23} \\
G_{12} &= \frac{y1}{u2} = \frac{-0.19s^7 + 0.47s^6 - 0.64s^5 + 0.54s^4 - 0.27s^3 + 0.095s^2 - 0.0154s - 0.0007}{s^8 - 3.555s^7 + 6.323s^6 - 7.5s^5 + 6.659s^4 - 4.711s^3 + 2.63s^2 - 1.06s + 0.23} \\
&\vdots \\
G_{87} &= \frac{y8}{u7} = \frac{5.6e5s^7 - 1.5e6s^6 + 2.6e6s^5 - 2.9e6s^4 + 2.6e6s^3 - 1.59e6s^2 + 6.7e5s - 8.5e4}{s^8 - 3.5s^7 + 6.323s^6 - 7.5s^5 + 6.659s^4 - 4.711s^3 + 2.635s^2 - 1.06s + 0.23} \\
G_{88} &= \frac{y8}{u8} = \frac{6.68e5s^7 - 1.15e6s^6 + 1.6e6s^5 - 2.02e6s^4 + 2.3e6s^3 - 1.6e6s^2 + 7.9e5s - 1.4e5}{s^8 - 3.55s^7 + 6.323s^6 - 7.5s^5 + 6.659s^4 - 4.71s^3 + 2.635s^2 - 1.06s + 0.23}.
\end{aligned}
\tag{10}
$$

Figure 15 illustrates the steps response of the open loop system with sampling time (3600 s). In this paper, 8 responses are simulated, instead of 64 responses (such as $G_{11}$, $G_{22}$, $G_{33}$, $G_{44}$, $G_{55}$, $G_{66}$, $G_{77}$, and $G_{88}$).

*5.2. Steady State Tracking.* It has been shown in this paper how state feedback control laws affect the transient response characteristics of a system, including the definition of freedom, specifying their own curves for a controllable equation of state, and how the eigenvalues affect the transient response. It has been demonstrated that, by adjusting the gain matrix $K$, only some of the transient parameters can be appropriately adjusted, but there is no control over the steady state value of the system. Next, the requirement for steady state monitoring for reference inputs is investigated. Such control systems are commonly referred to as servomechanisms.

Two approaches are described:

(i) Input gain, addition of an input gain to the state control law.

(ii) Integral, including an overall follow-up measure.

*5.2.1. Input Gain.* For the input gain $K_r$, presented in (8), the input gain controller is introduced to eliminate the stationary error associated with the complete status feedback controller for each constant input. The control law is designed such that the output $y(t)$ follows the reference input $r(t)$. The controller maintains tracking in steady state only if the reference inputs are stage inputs. The gain, $K$, is outside the feedback loop and makes the overall system sensitive to noise and disturbances. However, this is not "robust" since any change to the system parameter causes a nonzero error.

*5.2.2. Integral Action.* The technique of integral control is another type of technique of placing the poles. It is also known as a tracking controller when it needs an output to track the input control signal. The output feedback is transferred to the controlled system via the integrator. The integrator, also called integral action, is used to increase the system type and reduce finite errors to become zero [30].

The configuration of the integrated control technique is shown in Figure 16. The introduction of the input integrator causes the controller to have a pole at $S = 0$, which helps to eliminate the constant reference and improve the robustness of the system. However, Figure 16 shows the block diagram of a system with state feedback and integral control using MATLAB Simulink. Simulations are performed for a controller structure where a unit's step input is $[465 \;\; 459 \;\; 453 \;\; 471 \;\; 23.9 \;\; 22.9 \;\; 21.9 \;\; 24.9]$ and signals are used as the reference signal. To accomplish one of the design requirements, the output signals should follow the given reference signals. Through simulation, mathematical modeling for the system is verified and the performances for the controller structures are analyzed. Also, the initial state,

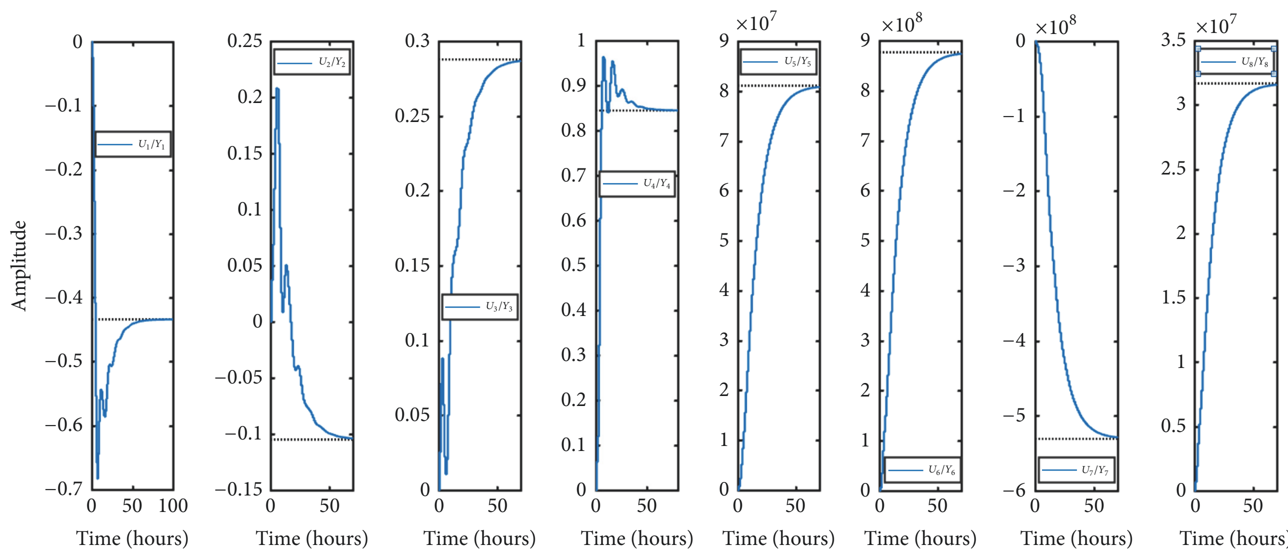


FIGURE 15: Steps response of the open loop system with sampling time of 3600 s.

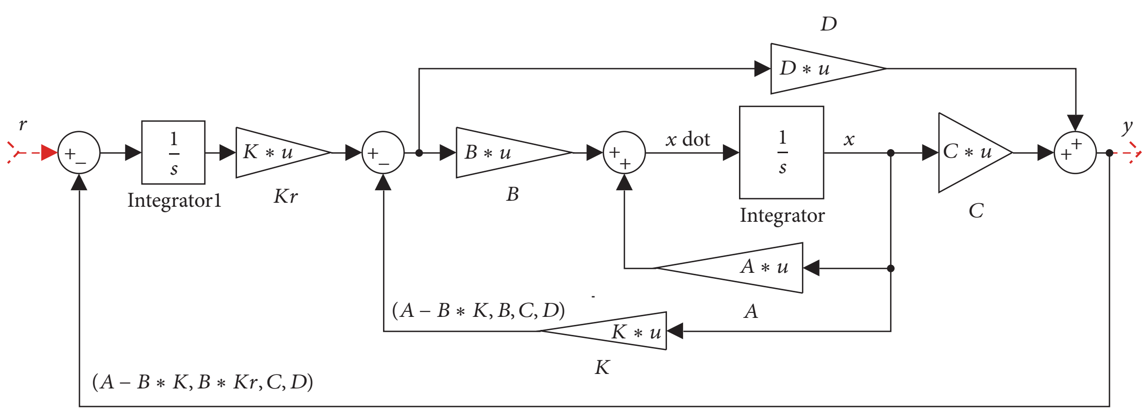


FIGURE 16: Block diagram of a system with state feedback and integral control using MATLAB Simulink.

$X_0$, of the system for concentrations and indoor temperatures is taken from measured data.

Simulation results of the system with a measured initial condition of $CO_2$ level are $X_0 = [446.4 \quad 440.6 \quad 435.44 \quad 453.4]$, and change set points to investigate the system's responses with state feedback control and integral action. The responses of the $CO_2$ level for the zones are illustrated in Figure 17.

Figure 18 shows the responses of the zones temperature with measured initial condition of the zone temperatures, $X_0 = [21.21 \quad 20.35 \quad 19.39 \quad 22.13]$.

For full state feedback controller, $K$, with input gain, $K_r$, and integral action, the steady state error is zero. Figure 19 illustrates the controller action (steady state error) of $CO_2$ level responses ($CO_2$-Er-Zones).

Figure 20 shows controller action (steady state error) of zones temperature responses (T-Er-Zones).

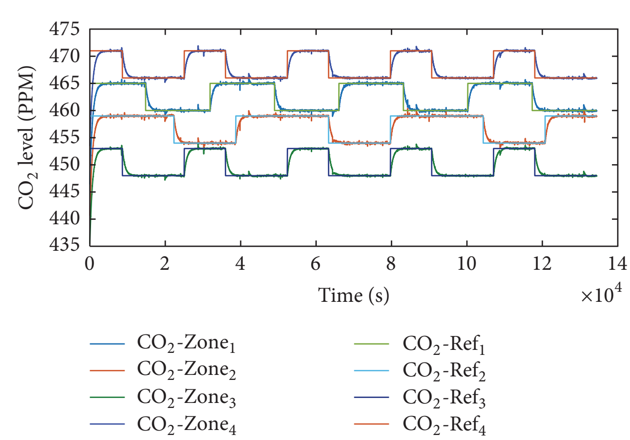


FIGURE 17: Outputs response of the $CO_2$ level for the zones $CO_2$-Zones with steps references $CO_2$-Refs.

## 6. Conclusion

In this paper, the HVAC system of the S. J. Carew building was modeled using the IDE ICE program. This model provides good approximation results in which hot water consumption and electricity consumption are compared with actual data.

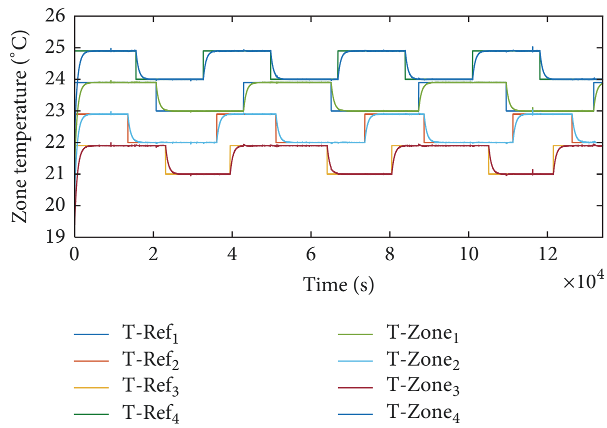


Figure 18: The outputs response of the zones temperature T-Zones with steps references T-Refs.

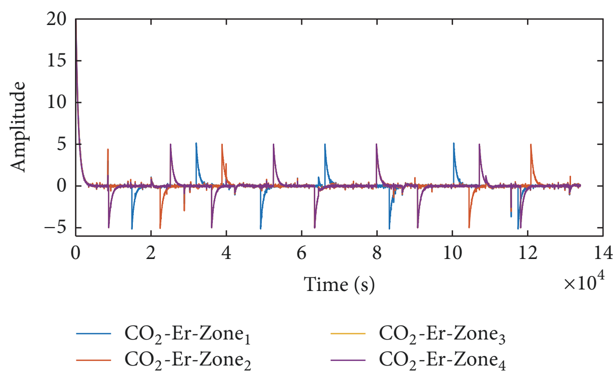


Figure 19: Controller action (steady state error) of $CO_2$ level responses for each zone $CO_2$-Er-Zones.

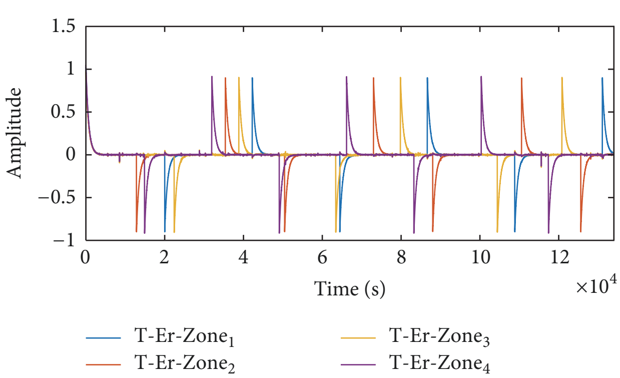


Figure 20: Controller action (steady state error) of temperature responses for each zone T-Er-Zones.

In addition, the outside temperature for the program and the measured data are compared for three months as the first part of the process. In the second part, the system identification toolbox was used to obtain the state space model of the multi-input and multioutput system MIMO. The model has eight status variables, eight inputs, and eight outputs, and model responses are within the permissible range. In the third part, a novel HVAC system model was developed that considers temperature and $CO_2$ concentration as the quantitative indices of comfort in a building. In applying an input-output feedback linearization method to linearize the HVAC system, one type of linear controller, pole placement controller with input gain, and integral action were able to regulate the linearized HVAC system at the desired set point without steady state error. Simulation results validated the proposed HVAC model, demonstrating its effectiveness in maintaining comfortable conditions.

## Conflicts of Interest

The authors declare that they have no conflicts of interest.

## Acknowledgments

This work is funded by the Ministry of Higher Education of Libyan Government, which is managed by CBIE in Canada. Also, The authors thank the Department of Facilities Management and Honeywell Office at Memorial University for providing them with structure details of the building and HVAC system.

## References

[1] American Society of Heating Refrigerating and Air-Conditioning Engineers, ASHRAE handbook, fundamentals, 2009.

[2] G. Lowry and M.-W. Lee, "Modelling the passive thermal response of a building using sparse BMS data," *Applied Energy*, vol. 78, no. 1, pp. 53–62, 2004.

[3] H. Madsen and J. Holst, "Estimation of continuous-time models for the heat dynamics of a building," *Energy and Buildings*, vol. 22, no. 1, pp. 67–79, 1995.

[4] M. J. Cunningham, "Inferring ventilation and moisture release rates from field psychrometric data only using system identification techniques," *Building and Environment*, vol. 36, no. 1, pp. 129–138, 2001.

[5] A. Mechaqrane and M. Zouak, "A comparison of linear and neural network ARX models applied to a prediction of the indoor temperature of a building," *Neural Computing and Applications*, vol. 13, no. 1, pp. 32–37, 2004.

[6] K. Peippo, P. Kauranen, and P. D. Lund, "A multicomponent PCM wall optimized for passive solar heating," *Energy and Buildings*, vol. 17, no. 4, pp. 259–270, 1991.

[7] EQUA Simulation AB, (January 2010): IDA Indoor Climate and Energy Version 4.7, http://www.equa.se/en/ida-ice.

[8] L. Ljung, *System Identification Theory for the User. Second Education*, Prentice Hall PTR, 2006.

[9] Q. Alvsv_ag, *HVAC systems Modeling, simulation and control for energy saving in HVAC-systems [M.S. thesis]*, Department of Engineering Cybernetics, Norwegian University of Science and Technology, 2001.

[10] Ljung, L. (n.d.). System identification toolbox 7, http://www.mathworks.com/help/pdf_doc/ident/ident.pdf.

[11] O. Tsakiridis, D. Sklavounos, E. Zervas, and J. Stonham, "A comfort-aware energy efficient hvac system based on the subspace identification method," *Journal of Energy*, vol. 2016, Article ID 5074846, 13 pages, 2016.

[12] D. Sklavounos, E. Zervas, O. Tsakiridis, and J. Stonham, "A subspace identification method for detecting abnormal behavior in

HVAC systems," *Journal of Energy*, vol. 2015, Article ID 693749, 12 pages, 2015.

[13] B. K. Hodge, *Analysis and Design of Energy Systems*, Prentice-Hall, Inc, Englewood Cliffs, NJ, USA, 1985.

[14] T. E. Mull, *HVAC Principles and Applications Manual*, McGraw-Hill New York, New York, NY, USA, 1998.

[15] G. Levermore, *Building Control Systems-CIBSE Guide*, Butterworth-Heinemann, Oxford, UK, 2000.

[16] M. Hordeski, *Control and Instrumentation Technology in HVAC: PCs and Environmental Controls*, CRC Press, Lilburn, GA, USA, 2000.

[17] A. Abdo-Allah, T. Iqbal, and K. Pope, "Modeling and analysis of an HVAC system for the S.J. Carew Building at Memorial University," in *Proceedings of the 30th IEEE Canadian Conference on Electrical and Computer Engineering, CCECE 2017*, IEEE, Windsor, Canada, May 2017.

[18] B. Tashtoush, M. Molhim, and M. Al-Rousan, "Dynamic model of an HVAC system for control analysis," *Energy*, vol. 30, no. 10, pp. 1729–1745, 2005.

[19] B. Argüello-Serrano and M. Vélez-Reyes, "Nonlinear control of a heating, ventilating, and air conditioning system with thermal load estimation," *IEEE Transactions on Control Systems Technology*, vol. 7, no. 1, pp. 56–63, 1999.

[20] J. Baek, E. Kim, and M. Park, "Adaptive Fuzzy Output Feedback Control for the Nonlinear Heating, Ventilating, and Air Conditioning System," in *Proceedings of the In Proceedings of the 23rd International Technical Conference on Circuits/Systems, Computers and Communications (ITC-CSCC*, pp. 1477–1480, Shimonoseki , Japan, 2008.

[21] E. Semsar, M. J. Yazdanpanah, and C. Lucas, "Nonlinear control and disturbance decoupling of an HVAC system via feedback linearization and back-stepping," in *Proceedings of the IEEE Conference on Control Applications*, vol. 1, pp. 646–650, IEEE, 2003.

[22] Z. Huaguang and L. Cai, "Decentralized nonlinear adaptive control of an HVAC system," *IEEE Transactions on Systems, Man, and Cybernetics, Part C (Applications and Reviews)*, vol. 32, no. 4, pp. 493–498, 2002.

[23] S. J. Emmerich and A. K. Persily, *State-of-the-Art Review of $CO_2$ Demand Controlled Ventilation Technology and Application*, Diane Publishing, Darby, PA, USA, 2001.

[24] X. Lu, T. Lu, and M. Viljanen, "Estimation of space air change rates and $CO_2$ generation rates for mechanically-ventilated buildings," in *Advances in Computer Science and Engineering*, M. Schmidt, Ed., In Tech, Rijeka, Croatia, 2011.

[25] M.-L. Chiang and L.-C. Fu, "Hybrid system based adaptive control for the nonlinear HVAC system," in *Proceedings of the 2006 American Control Conference*, p. 6, IEEE, Minneapolis, MN, USA, 2006.

[26] M. Chiang and L. Fu, "Adaptive Control of Switched Systems with Application to HVAC System," in *Proceedings of the 2007 IEEE International Conference on Control Applications*, IEEE, Singapore, 2007.

[27] D. A. Hodgson, *Investigation of a nonlinear controller that combines steady state predictions with integral action [Ph. D. thesis]*, Colorado State University, Fort Collins, CO, USA, 2010.

[28] H. Moradi, M. Saffar-Avval, and F. Bakhtiari-Nejad, "Nonlinear multivariable control and performance analysis of an air-handling unit," *Energy and Buildings*, vol. 43, no. 4, pp. 805–813, 2011.

[29] G. D. Pasgianos, K. G. Arvanitis, P. Polycarpou, and N. Sigrimis, "A nonlinear feedback technique for greenhouse environmental control," *Computers and Electronics in Agriculture*, vol. 40, no. 1–3, pp. 153–177, 2003.

[30] N. S. Nise, Ed., *Control System Engineering*, John Wiley & Sons, 2007.

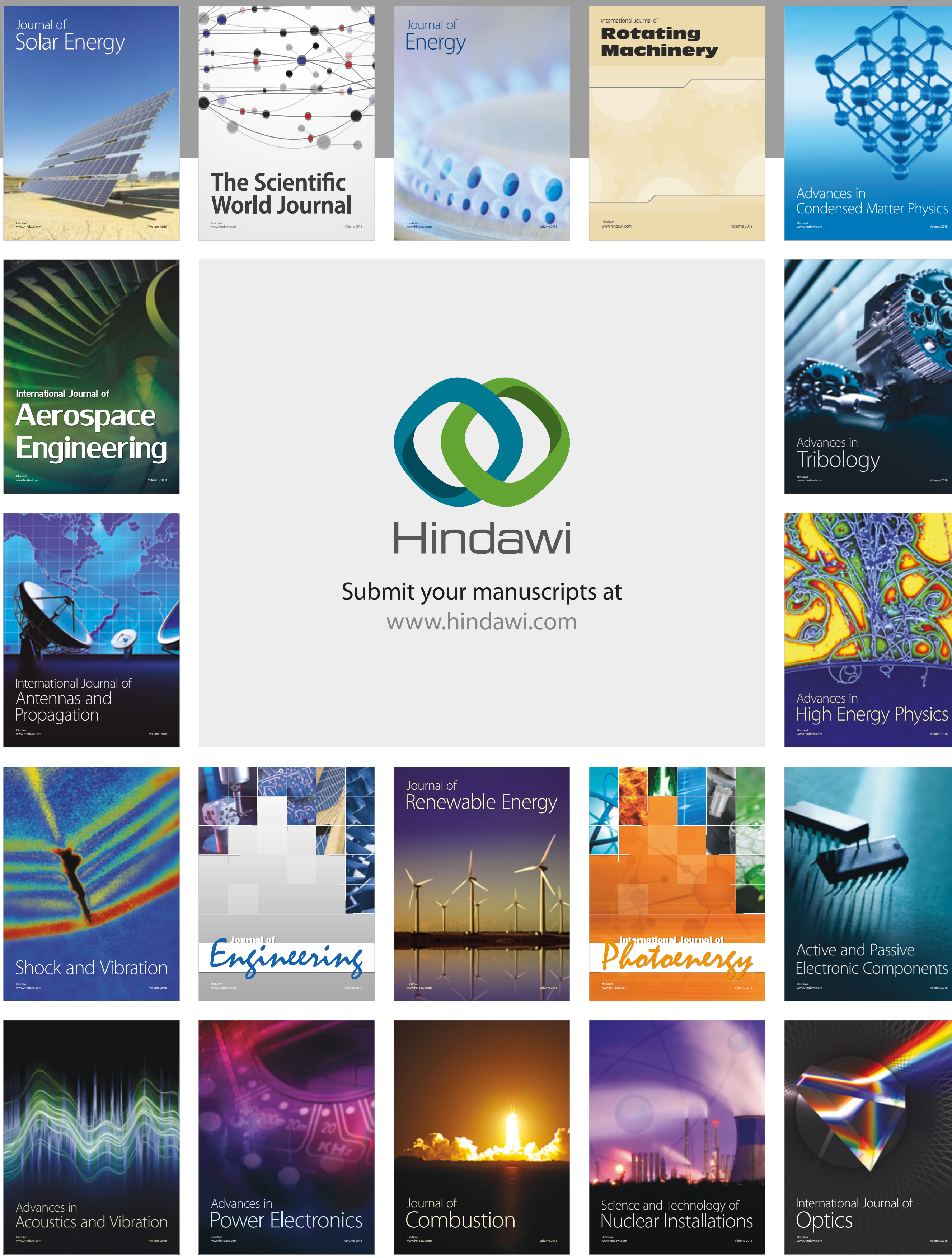
Journal of
Solar Energy
The Scientific
World Journal
Journal of
Energy
International Journal of
Rotating
Machinery
Advances in
Condensed Matter Physics
International Journal of
Aerospace
Engineering
Hindawi
Submit your manuscripts at
www.hindawi.com
Advances in
Tribology
International Journal of
Antennas and
Propagation
Advances in
High Energy Physics
Shock and Vibration
Journal of
Engineering
Journal of
Renewable Energy
International Journal of
Photoenergy
Active and Passive
Electronic Components
Advances in
Acoustics and Vibration
Advances in
Power Electronics
Journal of
Combustion
Science and Technology of
Nuclear Installations
International Journal of
Optics